



HAL
open science

Simple modelling and control of plasma current profile

François Delebecque, Jean-Pierre Quadrat, Sylvain Brémond, Emmanuel Witrant, Jean-François Artaud

► **To cite this version:**

François Delebecque, Jean-Pierre Quadrat, Sylvain Brémond, Emmanuel Witrant, Jean-François Artaud. Simple modelling and control of plasma current profile. CONTROLO 2008 - 8th Portuguese Conference on Automatic Control, Jul 2008, Vila Real, Portugal. pp.CD. hal-00329853

HAL Id: hal-00329853

<https://hal.science/hal-00329853>

Submitted on 13 Oct 2008

HAL is a multi-disciplinary open access archive for the deposit and dissemination of scientific research documents, whether they are published or not. The documents may come from teaching and research institutions in France or abroad, or from public or private research centers.

L'archive ouverte pluridisciplinaire **HAL**, est destinée au dépôt et à la diffusion de documents scientifiques de niveau recherche, publiés ou non, émanant des établissements d'enseignement et de recherche français ou étrangers, des laboratoires publics ou privés.

SIMPLE MODELING AND CONTROL OF PLASMA CURRENT PROFILE

François Delebecque^{**} Jean-Pierre Quadrat^{**}
Sylvain Brémond^{*} Emmanuel Witrant^{***}
Jean-François Artaud^{*}

^{*} INRIA-Rocquencourt, BP105 78150 Le Chesnay Cedex (France)

^{**} CEA-Cadarache, 13108 St Paul lez Durance Cedex (France)

^{***} GIPSA-Lab, Automatic Control department ENSIEG, BP46
38402 Saint Martin d'Hères Cedex (France)

Abstract: The purpose of this paper is to present a simplified model and control law of the current and temperature profile in a tokamak plasma. Based on a description of the plasma as a magnetised fluid, the model is expressed in the form of coupled one dimensional transport-diffusion equations. A simple feedback is used to obtain a given stationary profile. The numerical simulations are done in the Scilab/Scicos environment.

Keywords: plasma modeling, plasma control, tokamak

1. INTRODUCTION

A tokamak is a facility in which a plasma is magnetically confined and heated in order to produce nuclear fusion reactions. The magnetic confinement of the plasma particles in the vacuum vessel torus is obtained through the combination of toroidal and poloidal fields produced by external coils (see Figure 1) with the additional field produced by an electrical current flowing along the plasma ring. This plasma current is generally firstly generated by induction (the plasma ring can then be considered as the secondary loop of a transformer whose primary loop is the ohmic field coil (see Figure 1)). It allows to heat up the plasma, which behaves as a resistive conductor. But, in practice, ohmic heating and current drive do not allow to reach the adequate plasma temperature and duration required for future fusion reactors. Indeed the plasma resistivity decreases with temperature and technology limits the ohmic field coil current. Non inductive heating and current drive methods were thus developed to take it over, namely high power microwave or fast neutral beams injection.

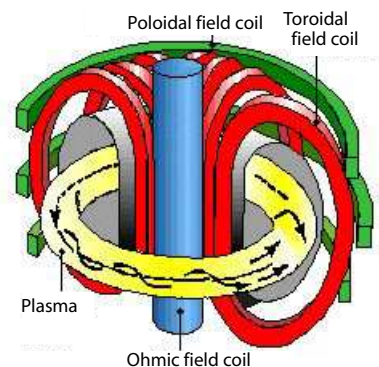


Fig. 1. Tokamak.

The control of tokamak plasma has a long history (see (Pironti and Walker, 2005) and related tutorials). In particular, four classes of control problems have been investigated:

- vertical stabilization of the plasma ring,
- control of the plasma ring shape,
- control of the magnetohydrodynamic (MHD) instabilities,

- control of the current, temperature and density profiles.

We are here concerned with the latter problem, which has been studied more recently in (Walker and al, 2006; Laborde, 2005; Moreau and al, 2006). The goal is to provide the operating conditions (in terms of profiles shapes) that are necessary to achieve advanced confinement schemes able to increase the fusion power production efficiency.

The profile control approaches cited above are mainly based on black box linear models where plasma physics is only used to select the set of relevant variables and the way they are coupled. These approaches require the identification of a MIMO system approximating the distributed physical system that is highly dependent on the operating conditions, which makes them costly in terms of experimentations. The first aim of this paper is to provide a simple PDE control-oriented model based on:

- the evolution of the resistive equation averaged on the magnetic surface as explained in (Blum, 1989),
- the experimental identification of some diffusion coefficients.

The second aim is to provide a simple control policy depending on the temperature providing a given current profile improving the fusion reaction. The feedback determines the energy profile that the set of antennas has to produce or to approach but does not give explicitly the effective control to apply.

Numerical experimentation have been performed in the Scilab-Scicos environment. Based on some experimental data, from the Tore Supra Tokamak the simulation results are compared with the outputs obtained by a more complex physics oriented code namely the Cronos software (Basiuk and al, 2003). Cronos is one of the main plasma integrated modeling codes, but it cannot be easily used in real-time or for control purposes.

In the second section, we recall the plasma physics background and the assumptions made to derive the distributed control-oriented model. The form used for the diffusion coefficients and the sources terms of the PDEs are detailed in the third section. They have been obtained by simplifying (Witran and al, 2007) after a sensibility analysis.

In the last section, the current profile control problem is set and solved.

2. TOKAMAK PLASMA PHYSICS

We recall here some basic physics background about the plasma macroscopic description on which the model is based.

2.1 Plasma magnetohydrodynamics

The dynamics of a plasma is governed by (see (Blum, 1989; Wesson, 2004)) the MHD equations:

$$\left\{ \begin{array}{l} \nabla \times E = -\partial_t B, \quad \text{Faraday's law,} \\ E + \zeta j_n + u \times B = \zeta j, \quad \text{Ohm's law,} \\ \nabla \cdot B = 0, \quad \text{B conservation,} \\ \nabla \times B = \mu_0 j, \quad \text{Ampère's law,} \\ \partial_t n + \nabla \cdot (nu) = n_s, \quad \text{particles conservation,} \\ mn \dot{u} + \nabla p = j \times B, \quad \text{momentum conservation,} \\ \frac{3}{2} \dot{p} + \frac{5}{2} p \nabla \cdot u + \nabla \cdot Q = p_s, \quad \text{energy conservation,} \\ p = knT, \quad \text{perfect gases law,} \end{array} \right.$$

where $\dot{v} \triangleq \partial_t v + v \cdot \nabla v$, E is the electric field, B is the magnetic field, u is the mean particles velocity, j is the current density, j_n is the non inductive current density, n is the particles density, p is the plasma pressure, T is the temperature, Q is the heat flux, m is the particle mass, μ is the magnetic permeability, ζ is the resistivity tensor, k is the Boltzmann constant, n_s is the particle source and p_s is the energy source.

2.2 Time Constants

In order to provide a model appropriate for plasma control studies, it is important to understand the time constants associated with the different physical phenomena at stake. We can bring out four time constants:

- The Alfvén time $\tau_A = a(\mu_0 mn)^{1/2}/B_0$, where a is the minor radius of the plasma ring and B_0 the toroidal magnetic field at the vacuum vessel center, is of the order of $10^{-6}s$ in present tokamaks.
- The density diffusion time $\tau_n = a^2/D$, where D is the particle diffusion coefficient, for modern tokamaks, is in the range 0.1s-1s;
- The heat diffusion time $\tau = na^2/K$, where K is the thermal conductivity coefficient is also in the range 0.1s-1s (3.4s for ITER);
- The resistive diffusion time constant $\tau_r = \mu_0 a^2/\zeta$ is of few seconds (100s-3000s for ITER).

The Alfvén time scale is used to describe the MHD instabilities phenomena, which are not considered here. Our model is focused on the dynamics of the resistive behavior of the plasma but a dynamical temperature species (electrons and ions) model is given. Due to the bad knowledge of the dynamics of species densities and the fact that online measurements are available, we suppose that they are given explicitly (in practice we use a filtered version of the ones given by the Cronos software).

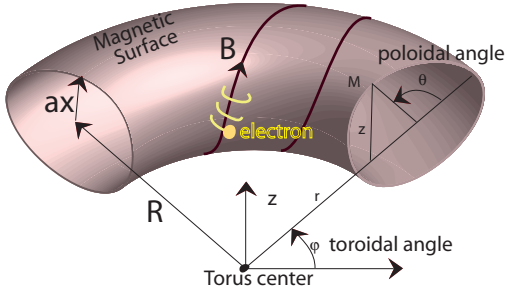


Fig. 2. Magnetic Surface.

2.3 Axisymmetry assumption

Due to the quasi symmetry of the magnetic configuration around the main axis of the facility, some simplified expressions can be derived.

From the conservation of B , it follows that there exists A such that $B = \nabla \times A$ with $A = (A_r, A_\varphi, A_z)$. Due to the axis symmetry, A is independent of the toroidal angle φ . Therefore $B_r = -(1/r)\partial_z(rA_\varphi)$ and $B_z = (1/r)\partial_r(rA_\varphi)$. In the following rA_φ will be denoted Ψ .

Denoting by $\mathcal{D}(r, z)$ the horizontal disk centered on the z -axis with its boundary passing through the point M (with coordinates (r, z)) the Stoke's formula applied to \mathcal{D} and the field B :

$$2\pi\Psi = 2\pi r A_\varphi = \int_{\partial\mathcal{D}} A = \int_{\mathcal{D}} \nabla \times A = \int_{\mathcal{D}} B,$$

gives the interpretation of Ψ as the poloidal magnetic flux. Similarly, applying Stoke's to \mathcal{D} and the field j , using Ampère's law and denoting rB_φ by f we have:

$$2\pi f = 2\pi r B_\varphi = \int_{\mathcal{D}} \partial B = \int_{\mathcal{D}} \nabla \times B = \mu_0 \int_{\mathcal{D}} j.$$

From Ampère's law and the definition of Ψ we have:

$$j_\varphi = \frac{\partial_z B_r - \partial_r B_z}{\mu_0} = L\Psi \triangleq -\frac{1}{\mu_0} \left[\partial_z \frac{\partial_z \Psi}{r} + \partial_r \frac{\partial_r \Psi}{r} \right]$$

To sum up,

$$B = \left(-\frac{\partial_z \Psi}{r}, \frac{f}{r}, \frac{\partial_r \Psi}{r} \right), \quad (1)$$

$$j = \left(-\frac{\partial_z f}{\mu_0 r}, L\Psi, \frac{\partial_r f}{\mu_0 r} \right). \quad (2)$$

2.4 Magnetic Surfaces and Associated Quantities

We are interested in the dynamics of the current density profile, i.e., phenomena at the resistive time scale. At this time scale, we can consider that the momentum equation is at the equilibrium i.e. :

$$\nabla p = j \times B.$$

This equation yields $B \cdot \nabla p = 0$ and $j \cdot \nabla p = 0$, and therefore the magnetic field lines and the current

lines lie in the so called *magnetic surface* which are surfaces of constant pressure. The magnetic surfaces form a set of nested toroids as in Figure 2. The torus symmetry implies that $\partial_\varphi p = 0$. The magnetic field B being orthogonal to ∇p we have $-\partial_r p \partial_z \Psi + \partial_z p \partial_r \Psi = 0$ which means that ∇p is proportional to $\nabla \Psi$, thus Ψ is constant on a magnetic surface. We can show using the orthogonality of j with ∇p that f is constant on the magnetic surfaces, as it has been done for Ψ .

Using (1),(2) and the colinearity of $\nabla \Psi$, ∇f , and ∇p

$$\nabla p = j \times B = \frac{L\Psi}{r} \nabla \Psi - \frac{f}{\mu_0 r^2} \nabla f,$$

which gives the plasma equilibrium Grad-Shafranov equation :

$$L\Psi = r \partial_\Psi p + \frac{1}{2\mu_0 r} \partial_\Psi (f^2).$$

Given that many physics quantities are constant over magnetic surfaces, it was found very useful to define an averaging method of any quantity over a magnetic surface in order to finally get 1D equations. In the following of this section the magnetic surface will be indexed by the parameter ρ .

We define (see (Blum, 1989)) $\langle A \rangle \triangleq \partial_\nu \int_{\mathcal{V}} A d\mathcal{V}$ with \mathcal{V} the volume inside the magnetic surface.

Denoting $v' = \partial_\rho \mathcal{V}$, it can be shown that:

$$\langle \nabla \cdot A \rangle = \partial_\nu \langle A \cdot \nabla \mathcal{V} \rangle = \frac{1}{v'} \partial_\rho (v' \langle A \cdot \nabla \rho \rangle),$$

A particular indexing choice of the magnetic surface corresponds to the following definition of ρ :

$$\rho \triangleq \sqrt{\frac{\Phi}{\pi B_0}}, \quad (3)$$

where B_0 is the toroidal magnetic field at the vacuum vessel center (which is assumed to be constant) and

$$\Phi \triangleq \int_{\mathcal{S}} B d\mathcal{S} = \frac{1}{2\pi} \int_{\mathcal{V}} \frac{B_\varphi}{r} d\mathcal{V} = \frac{1}{2\pi} \int_{\mathcal{V}} \frac{f}{r^2} d\mathcal{V}, \quad (4)$$

where \mathcal{S} denotes a poloidal section of a magnetic surface and \mathcal{V} the volume enclosed by this magnetic surface.

It has the dimension of a length. In a first approximation, it can be seen as the mean geometrical radius of the magnetic surface since the toroidal field applied from outside the plasma is very large compared with the toroidal field (produced by the plasma by the diamagnetic and/or paramagnetic effects).

The *security factor* is defined by

$$q \triangleq -\frac{1}{2\pi} \frac{\partial \Phi}{\partial \Psi}.$$

Higher values of q lead to greater plasma stability, and specific q profiles can be related to higher core confinement thus it is an important output plasma variable.

2.5 Resistive Diffusion Equation

Note that since Ψ and f are constant on each magnetic surface there exists $\bar{\Psi}$ and \bar{f} such that $\Psi(r, z) = \bar{\Psi}(\rho(r, z))$ and $f(r, z) = \bar{f}(\rho(r, z))$.

It can be shown after some calculation (see (Blum, 1989; Imbeaux and al, 2006)) that

$$\partial_t \bar{\Psi} = -\frac{\langle E.B \rangle}{\bar{f} \langle 1/r^2 \rangle}$$

Now, using Ohm's law we have $\langle E.B \rangle = \eta \langle (j - j_n).B \rangle$

Therefore we obtain (see (Blum, 1989; Imbeaux and al, 2006)) :

$$\partial_t \bar{\Psi} = \frac{\eta \bar{f}}{\mu_0 c_3} \partial_\rho \left(\frac{c_2}{\bar{f}} \partial_\rho \bar{\Psi} \right) + \frac{\eta \langle j_n.B \rangle}{\bar{f} \langle 1/r^2 \rangle}, \quad (5)$$

with

$$c_2(\rho) = v' \langle |\nabla \rho|^2 / r^2 \rangle, \quad c_3(\rho) = v' \langle 1/r^2 \rangle.$$

Using (4) and (3) we have :

$$\partial_\rho \Phi = \frac{\bar{f} v'}{2\pi} \langle 1/r^2 \rangle = 2\pi \rho B_0,$$

and therefore

$$\bar{f} = \frac{4\pi^2 \rho B_0}{c_3}.$$

Substituting \bar{f} by its value in (5) we obtain the *resistive equation* :

$$\partial_t \bar{\Psi} = \frac{\eta \bar{f}}{\mu_0 c_3^2} \partial_\rho \left(\frac{c_2 c_3}{\rho} \partial_\rho \bar{\Psi} \right) + \frac{\eta v' \langle j_n.B \rangle}{4\pi^2 \rho B_0}. \quad (6)$$

By symmetry, the boundary condition at $\rho = 0$ is

$$\partial_\rho \bar{\Psi}(0) = 0. \quad (7)$$

The boundary condition at $\rho = \rho_{\max}$ is obtained by computing I , the total toroidal plasma current (see (Blum, 1989; Imbeaux and al, 2006)) which gives :

$$\partial_\rho \bar{\Psi}(\rho_{\max}) = \frac{-2\pi \mu_0 I}{c_2}. \quad (8)$$

Note that $V = \dot{\Psi}$ can also be used as a boundary condition.

In the sequel, we will assume that the magnetic surfaces are time constant, that \mathcal{S} is a disk, and that $\varepsilon \triangleq \rho/R$ (where R is the *major radius*) is small.

3. RESOLUTION OF THE DIFFUSION RESISTIVE MODEL

In this section we specify the resistive equation by making some assumption on magnetic surface shapes and by giving empirical formula for the resistivity η , bootstrap current and lower hybrid current which drive the non inductive profile. Only two sources of non inductive current are considered here the bootstrap and lower hybrid currents. We solve the corresponding resistive equation using the ODE solver of Scilab-Scicos and compare the results obtained with those computed by Cronos. The model proposed here is a simplified version of the model introduced in (Witrant and al, 2007). The simplification has been obtained empirically by studying the sensibility of the parameters introduced and studying their contribution to error with results obtained by Cronos on three shots.

3.1 Geometric Hypotheses

In the following we write the diffusive equation under the cylindric hypothesis. We consequently assume that $\varepsilon = a/R$ is small and that the corresponding poloidal sections are circular. Under these assumptions we have :

$$v' = 4\pi^2 R \rho, \quad c_2 = c_3 = \frac{4\pi^2 \rho}{R}, \quad \langle |\nabla \rho|^2 \rangle = 1,$$

$$\frac{\eta v' \langle j_n.B \rangle}{4\pi^2 \rho B_0} = \eta R j_n.$$

e	electric electron charge
i	ion electron charge
m_e	electron mass
m_i	average ion mass (kg)
Z	effective ion electron charge ratio
μ_0	permeability of free space (H/m)
ε_0	permittivity of free space (F/m)
R	major radius of the plasma (m)
a	minor radius of the plasma
B_0	toroidal magnetic field at the plasma center
I	total plasma current (A)
V	loop voltage

Table 1. Primitive Constants

During the heating process, antennas are used (here the numerical experiments will be done only with the lower hybrid antenna (LHCD)) and the dynamic equation of the magnetic flux is :

$$\begin{cases} \partial_t \bar{\Psi} = R\eta(T_e) (j_b(\partial_x P_e, \partial_x \bar{\Psi}) + j_h + c_j \frac{1}{x} \partial_x (x \partial_x \bar{\Psi})), \\ \partial_x \bar{\Psi}(t, 0) = 0, \quad \partial_x \bar{\Psi}(t, 1) = -c_I I(t), \end{cases} \quad (9)$$

where :

- $-c_j \frac{1}{x} \partial_x (x \partial_x \bar{\Psi})$, denoted $j_\varphi(\bar{\Psi}, t)$, is the toroidal current plasma profile,

v	$2\pi^2 a^2 R$ plasma ring volume
c_j	$2\pi^2/\mu_0 v$
c_I	$R\mu_0/2\pi$
c_q	$a^2 B_0$
c_D	$0.09 m_e/m_i$
c_τ	$4.8 \cdot 10^{14} i/e(1000e)^{1.5}$
c_e^χ	$2.510^{-4} a/eB_0$
c_i^χ	$2.510^{-4} a/eB_0$
c_Z^η	$3.37 \cdot 10^{-33} Z(0.73 + 0.27Z)/(0.53 + 0.47Z)$
c_η	10 (estimated)
c_b	$0.70 R\sqrt{x}$
c_x^η	$8 + 10\sqrt{x(1-x)}$

Table 2. Derived constants.

(r, φ, z)	cylindric coordinates
$\bar{\Psi}$	magnetic flux profile of the poloidal field
Φ	magnetic toroidal flux
A	magnetic potential
B	magnetic field
j_b	bootstrap current density profile
j_h	hybrid current density profile
j_φ	toroidal current density profile
q	safety factor profile
q^*	wanted safety factor profile
T_e	electron temperature profile(J)
n_e	$c_e^n(2 - \sqrt{1 + 3x^2}) + c_e^\nu$ electron density profile
P_e	$n_e T_e$ electron pressure profile
T_i	ion temperature profile(J)
n_i	$c_i^n(2 - \sqrt{1 + 3x^2}) + c_i^\nu$ ion density profile
P_i	$n_i T_i$ ion pressure profile
τ_e	electron collision time
τ_i	ion collision time
η	plasma resistivity profile
χ_e	electronic temperature diffusion
χ_i	ion temperature diffusion
ε	a/R inverse aspect ratio
ρ	magnetic surface coordinate
x	ρ/a normalized magnetic surface coordinate
\mathcal{V}	volume inside the magnetic surface

Table 3. Main notations

- j_h is the current deposit coming from the lower hybrid effect antenna,
- j_b is the bootstrap current described later,
- c_j is a constant,
- I is a total plasma current.

3.2 Resistivity

There exist many models of resistivity. It turns out that, in view of the numerical results shown in subsection 3.8, the following simple formula :

$$\eta = c_Z^\eta c_x^\eta / T_e^{3/2}. \quad (10)$$

is sufficiently accurate for our purpose. More precise formulas are given in (Wesson, 2004) Section-14.10. The difference with the one we use here is not significant on the current profile on the Tore Supra shots on which we test our model.

3.3 Temperature Profile

To determine the resistivity we need a temperature model. We use the following simplified dynamics for describing the electronic temperature T_e and ion temperature T_i evolutions :

$$\begin{aligned} \frac{3}{2} \partial_t (n_e T_e) &= 1/(a^2 x) \partial_x (x \chi_e \partial_x T_e) - \frac{c_D n_e (T_e - T_i)}{\tau_{ei}} \\ &\quad + c_\eta \eta j_\varphi (j_\varphi - j_b - j_h) + \rho_h j_h, \\ \frac{3}{2} \partial_t (n_i T_i) &= 1/(a^2 x) \partial_x (x \chi_i \partial_x T_i) - \frac{c_D n_e (T_i - T_e)}{\tau_{ei}}, \end{aligned}$$

with

$$\tau_{ei} = c_\tau T_e^{1.5} / n_i,$$

$$\chi_e = c_e^\chi n_e q^2 \partial_x T_e, \quad \chi_i = c_i^\chi n_i q^2 \partial_x T_i,$$

where the species densities n_e and n_i are supposed to be given (in fact provided by Cronos software).

To improve this model a term of radiating loss will be added in future numerical experiments.

3.4 Bootstrap Current

The bootstrap current comes from a complex mechanism where some particles do not follow the magnetic field but are trapped in a plasma zone. The contribution of the electron (only considered here) to the induced current is given by :

$$j_b(\partial_x P_e, \partial_x \bar{\Psi}) = c_b \frac{\partial_x P_e}{\partial_x \bar{\Psi}}.$$

In (Wesson, 2004) Section-14.12 we can find more precise formulas where the bootstrap depends not only of P_e but also P_i , T_e and T_i in the future we will look more precisely to the influence of the other terms.

3.5 Lower Hybrid Current Drive

To be able to evaluate the quality of the proposed model for the plasma control, we need to compare the result obtained with experiments. For that the lower hybrid heating antenna deposit used is a simplified version of the one given in (Witrant and al, 2007). In the control part we will not used this particular current deposit but will consider an arbitrary coupled current-heating deposit that the set of antennas available will have to approximate.

3.6 Security Factor

The security factor can be rewritten as :

$$q(t, x) = \frac{-c_q x}{\partial_x \bar{\Psi}(t, x)}. \quad (11)$$

Typically, we control the plasma current density profile using the heating antenna source j_h and the

flux variation at the plasma edge I . We would like to obtain and stabilize a specified security factor profile q^* appropriate for fusion conditions, under the constraint of securing the plasma stability.

3.7 Scilab/Scicos Implementation

This partial differential equation model has been solved numerically using the free software Scilab. The equation is solved using the default ode solver of Scilab. The state derivatives are approximated by appropriate finite difference matrices. The simulation is done by a script function or implemented using the Scicos block-diagram editor (see Figure3). The ode solver uses multistep formulas and the numerical results are obtained within a few seconds.

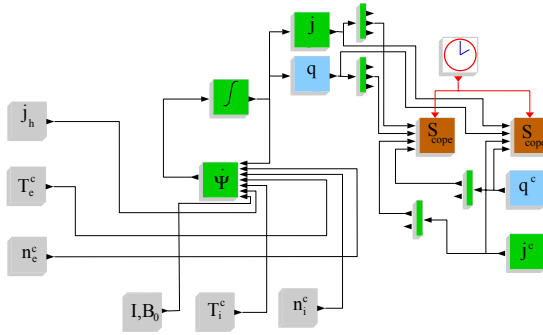


Fig. 3. Scicos Diagram for Magnetic Flux Integration.

3.8 Numerical Results

The numerical results obtained are compared to those obtained by the Cronos software from experimental datas coming from a typical Tore Supra shot. Cronos is a set of Matlab programs dedicated to the simulation and the experimental data processing of the plasma transport phenomenon. It contains the description of the actuator interaction with the plasma. The simulation obtained by the simplified model described here uses the Cronos data for the unmodeled states (the species densities).

Figure-4-5 compares the Cronos and the proposed model simulation results. We see that the model seems to give enough information to have an overview of the tracking control quality.

4. CURRENT DENSITY PROFILE CONTROL

In this section we describe how to stabilize the security profile around a specific value which corresponds to an improved temperature profile for the fusion purpose. For that we can use several

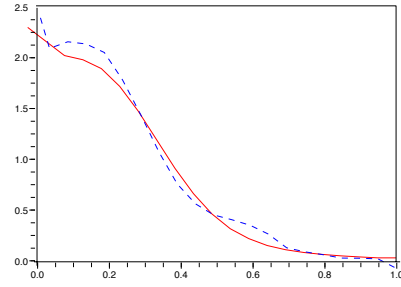


Fig. 4. Current profile at the shot end (red line model, blue dotted line Cronos).

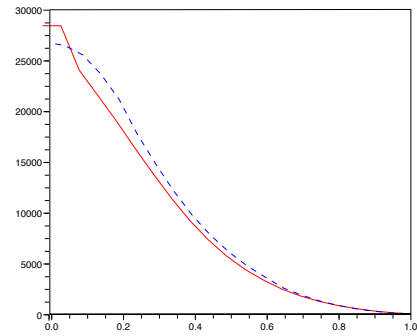


Fig. 5. Electron pressure profile at the shot end (red line model, blue dotted line Cronos).

heating and current deposit antennas. Each antenna has its specific profile deposit. We suppose that with all these means we are able obtain any current shape deposit. Clearly, this is a strong hypothesis only suitable for a preliminary study. This hypothesis means that any shape can be approximated with the available antennas.

4.1 Remarks on tracking control

Let us consider the following linear system

$$\begin{cases} \dot{x} = Ax + By + u \\ \dot{y} = Cx + Dy + Eu \end{cases}$$

and let us suppose that we want that the state x tracks asymptotically x^* that is :

$$\lim_{t \rightarrow \infty} x(t) = x^*$$

The feedback

$$u = -(Ax^* + By),$$

leads to the closed loop system :

$$\begin{cases} \dot{x} = A(x - x^*) \\ \dot{y} = Cx - EAx^* + (D - EB)y \end{cases}$$

which achieves the desired tracking. Of course the above control is valid only if both A and $D - EB$ are asymptotically stable.

Necessary and sufficient condition for tracking control models with more natural assumptions

are given in (Francis, 1977) and (Isidori and Byrnes, 1990) but are difficult to implement in the plasma model.

4.2 Security factor profile tracking

We can apply the tracking feedback of the previous section to the plasma magnetic flux in (9) where $\bar{\Psi}$ play the role of x and (T_e, P_e) the role of y and j_h the role of u . Moreover, let us suppose that we want a specific security profile q^* which corresponds to $\bar{\Psi}^*$ defined up to an additive constant.

Let us take for example :

$$q^* = c_g \max \left[1, e^{3(x-0.3)} \right],$$

where c_g is chosen in such way that the magnetic flux boundary condition at $x = 1$ is satisfied.

Since asymptotically in time $\partial_t \bar{\Psi} = V$ where V is the loop voltage, we obtain a q^* tracking control called j_h as a feedback on the pressure from (9) :

$$j_h = -j_b \left[\partial_x P_e, \frac{-c_q x}{q^*} \right] - c_j \frac{1}{x} \partial_x \left[x \partial_x \left[\frac{-c_q x}{q^*} \right] \right] + \frac{V}{R\eta[T_e]}$$

This control is easy to implement because it does not need a model for the temperature and the pressure. This point is very useful since, for the time being, there does not exist good model for these quantities.

To slow down the influence of the tracking feedback we use a time varying gain $G(t)$ starting from zero at time 0 and converging to one with time going to infinity.

Governed by this feedback the magnetic flux admits the dynamics :

$$\partial_t \bar{\Psi} = R\eta(T_e) \left(j_b + G(t) j_h + c_j \frac{1}{x} \partial_x (x \partial_x \bar{\Psi}) \right).$$

We observe numerically (with the simplify temperature and densities model) that the desired equilibrium is stable see Figure-6. The current profile obtained is not smooth because the target is not smooth. More smooth current profile can be obtained. The sensibility of the current and the pressure with the security factor target is high and will be explore in future work.

5. CONCLUSION

Based on a resistive model of the current in the plasma a simple tracking of a desired security factor profile has been obtained. The simulation results are encouraging. The next step is to generate the current deposit determined by the tracking feedback using the available antennas. The sensibility analysis of the security factor with respect

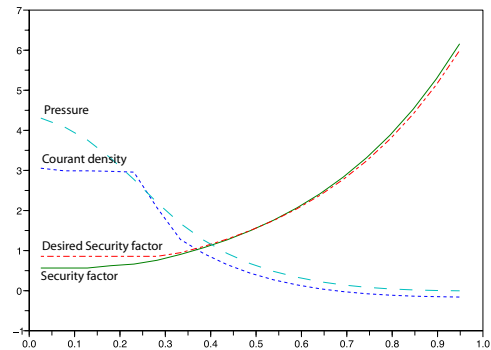


Fig. 6. Comparison of the security factor and the target at final time.

to the control shape deposit will be an important issue since the available shape space obtained using the existing antenna set is limited. Other validations of the proposed feedback with better models will be also an important issue. Finally, a proof of stability of the closed loop nonlinear PDE system would be very useful.

6. REFERENCES

- Basiuk, V. and al (2003). Simulations of steady-state scenarios for tore supra using the cronos code. *Nuclear Fusion*.
- Blum, J. (1989). *Numerical Simulation and Optimal Control in Plasma Physics*. Gauthier-Villars.
- Francis, B.A. (1977). The linear multivariable regulator problem. *SIAM Control*.
- Imbeaux, F. and al (2006). Cronos user's guide. Technical Report PHY/NTT-2006.002. CEA. Cadarache (France).
- Isidori, A. and C. Byrnes (1990). Optimal regulation of nonlinear systems. *IEEE-AC*.
- Laborde, L. (2005). Contrôle des profils de courant et de pression en temps réel dans les plasmas de tokamaks. PhD thesis. Provence University (France).
- Moreau, D. and al (2006). New dynamic-model approach for simultaneous control of distributed and kinetic parameters in the iterlike jet plasmas.
- Pironti, A. and M. Walker (2005). Fusion, tokamak and plasma control. In: *Special Issue on Fusion* (Control System Magazine, Ed.). IEEE.
- Walker, M. L. and al (2006). Emerging applications in tokamak plasma control. In: *Special Issue on Fusion* (Control System Magazine, Ed.). IEEE.
- Wesson, J. (2004). *Tokamaks*. Oxford Scienc Publications.
- Witrant, E. and al (2007). A control oriented model of the flux diffusion in tokamak plasma. *Phys. Cont. Fusion* **7**, 1075–1105.